

NUMERICAL SIMULATION OF RESONANT TUNNELING OF FAST SOLITONS FOR THE NONLINEAR SCHRÖDINGER EQUATION

WALID K. ABOU SALEM¹, XIAO LIU² AND CATHERINE SULEM²

ABSTRACT. In a recent paper [4], we showed that the phenomenon of resonant tunneling, well known in linear scattering theory, takes place for fast solitons of the Nonlinear Schrödinger (NLS) equation in the presence of certain large potentials. Here, we illustrate numerically this situation for the one dimensional cubic NLS equation with two classes of potentials, namely the ‘box’ potential and a repulsive 2-delta potential under certain conditions. In particular, we show that the transmitted wave is close to a soliton, calculate the transmitted mass of the solution and show that it converges to the total mass of the solution as the velocity of the soliton is increased.

1. INTRODUCTION

The effective dynamics of coherent structures (solitary waves) for Nonlinear Schrödinger (NLS) equations with or without external potential has been the object of numerous studies in the last twenty years. Typically, in the neighborhood of stable states, the dynamics reduces to the coupling of two systems: a finite-dimensional system for the evolution of parameters characterizing the soliton, and an infinite-dimensional one governing the radiation of energy to spatial infinity. For a soliton moving in a slowly varying external potential, [1, 6, 7, 8, 10], or in the presence of rough yet small (nonlinear) perturbations, [2, 9], the long time dynamics of the center of mass of the soliton behaves like a *classical* particle in an effective potential that corresponds to the restriction of the potential or perturbation to the soliton manifold. On the other hand, there are situations such as the “*blind*” collision of two fast solitons in an external potential, [3], or the scattering of solitons with high velocity by a delta impurity, [11], where quantum effects dominate. In the latter reference, the authors show that the incoming soliton splits into two waves, a reflected one and a transmitted one, each being a single soliton, and the transmitted rate is well approximated by the quantum transmission rate of linear scattering from a single delta potential.

In a recent work [4], we showed that the phenomenon of *resonant tunneling*, referring to a well known situation in linear scattering theory where incoming waves through potential barriers are fully transmitted at certain energies, can occur for nonlinear equations in certain limiting cases. More

precisely, we considered the NLS equation in one dimension

$$(1.1) \quad \begin{cases} i\partial_t u = Hu + f(u) \\ u(x, 0) = u_0(x) \end{cases}$$

where $H = -\frac{1}{2}\partial_x^2 + V$, and V is an external potential. The hypotheses on the nonlinearity are essentially those sufficient for existence of a global smooth solution and existence of (orbitally) stable solitary waves solutions, which include both Hartree and power nonlinearities. The assumptions on the potential V is that it is bounded and compactly supported, such that the resolvent $R_V(\lambda) = (H - \lambda^2)^{-1}$ has no poles for $\Im\lambda > 0$. Also, for $\lambda \in \mathbb{R} \setminus \{0\}$, the equation

$$(H - \lambda^2)u = 0$$

has unique solutions $e_{\pm}(x, \lambda)$ satisfying

$$(1.2) \quad e_{\pm}(x, \lambda) = \begin{cases} e^{\pm i\lambda x} + R(\lambda)e^{\mp i\lambda x}, & \pm x < -l, \\ T(\lambda)e^{\pm i\lambda x}, & \pm x > l, \end{cases}$$

for some $l > 0$. The transmission and reflection coefficients $T(\lambda)$ and $R(\lambda)$ respectively, satisfy the unitary condition

$$|T(\lambda)|^2 + |R(\lambda)|^2 = 1,$$

and are differentiable in $\lambda \in \mathbb{R} \setminus \{0\}$, with

$$|\partial_{\lambda} T|, |\partial_{\lambda} R| = O(l + q^{-1}),$$

where l depends on V , and q measures the size of the potential. The key hypothesis concerns *resonant tunneling*: We assume that there exists $\lambda_0 \in \mathbb{R} \setminus \{0\}$ that depends on V such that $R(\lambda_0) = 0$.

Taking as initial condition a soliton of the NLS equation (without potential) centered at $a_0 \ll 0$ and moving from the left at velocity $v \gg 1$, we showed rigorously the heuristic intuition that the dynamics can be decomposed in three phases: (i) the pre-collision phase, corresponding to $t \in [0, t_1 = \frac{|a_0| - v^{\eta}}{v}]$, (ii) the collision phase for $t \in [t_1, t_2 = \frac{|a_0| + v^{\eta}}{v}]$ and the post-collision phase $[t_2, t_3 = t_2 + \sigma \ln v]$, for some parameters $\eta \in (0, 1)$ and $\sigma > 0$. In the pre- and post collision regime, the soliton is not affected by the potential, and the dynamics approximately follows that of the NLS equation (without potential). In the intermediate regime, the dynamics is approximated by the linear flow due to the high velocity v of the moving soliton and consequently short time interaction. Notice that the size of the potential q is arbitrarily large.

The purpose of this note is to illustrate numerically this phenomenon in the context of the focusing cubic NLS equation ($f(u) = -|u|^2 u$) in one space dimension with two examples of external potentials V where resonant tunneling may take place: $V(x)$ is a double delta potential of height $q > 0$ and located at points $\pm l$:

$$(1.3) \quad V(x) = q(\delta(x + l) + \delta(x - l))$$

and $V(x)$ is a box potential, of height q and width $2l$:

$$(1.4) \quad V(x) = q(\Theta(x+l) - \Theta(x-l))$$

where Θ is the Heaviside step function. We note that (1.1) is globally well-posed in H^1 for the above choice of potentials and nonlinearity.

In the absence of the external potential ($V = 0$), the NLS equation (1.1) with focusing cubic nonlinearity admits solitary wave solutions of the form

$$u(x, t) = Ae^{i\phi_0 + ivx + i\frac{A^2 - v^2}{2}t} \operatorname{sech}(A(x - a_0 - vt))$$

where $a_0 \in \mathbb{R}$ is the initial center of mass position of the soliton, $v \in \mathbb{R}$ is its velocity, $\phi_0 \in [0, 2\pi)$ is the phase, and $A \in \mathbb{R}^+$.

Generally, the NLS equation (1.1) with external potential V is invariant under global gauge transformations, which leads to the conservation of mass or charge

$$M = \int dx |u|^2.$$

Furthermore, since the potential V is time-independent, (1.1) is invariant under time-translations, which implies conservation of the energy functional

$$E(u) = \int dx \left(\frac{1}{2} |\nabla u|^2 - \frac{1}{2} |u|^4 + V|u|^2 \right).$$

We will use those invariants to check the accuracy of our numerical scheme.

The paper is organized as follows. In Section 2 we recall some basic facts about linear scattering theory and apply it to the two examples of potential under consideration. In Section 3, we describe the numerical method and some tests to validate the computations. In Section 4, we give a detailed description of our numerical results.

2. LINEAR SCATTERING THEORY

The two families of potentials above satisfy the required hypotheses. We will refer to the $2\text{-}\delta$ potential (1.3) as potential (P1), and to the box potential (1.4) as potential (P2).

In the case of potential (P1), the reflection and transmission coefficients in the solutions (1.2) have the form

$$(2.1) \quad R(\lambda) = q \frac{-ie^{-2il\lambda}(\lambda(1 + e^{4il\lambda}) + iq(1 - e^{4il\lambda}))}{\lambda^2 + 2i\lambda q - q^2 + e^{4il\lambda}q^2}$$

$$(2.2) \quad T(\lambda) = \frac{\lambda^2}{\lambda^2 + 2i\lambda q - q^2 + e^{4il\lambda}q^2}$$

The numerator of $R(\lambda)$ identifies to $-2iq(\lambda \cos(2l\lambda) + q \sin(2l\lambda))$. Thus, if λ_0 is such that $\tan(2l\lambda_0) = -\lambda_0/q$, $R(\lambda_0) = 0$ and resonant tunneling occurs. In the NLS equation, the role of the wave number λ is played by the velocity, which is assumed to be large. Therefore, we will choose our parameters so that the velocity v of the initial solitary wave satisfies $\frac{v}{q} = -\tan(2lv)$.

In the case of the potential (P2), the reflection and transmission coefficients in the solutions (1.2) have the form

$$(2.3) \quad R(\lambda) = q \frac{ie^{-2i\lambda} \sin(2l\sqrt{\lambda^2 - 2q})}{\cos(2l\sqrt{\lambda^2 - 2q})\lambda\sqrt{\lambda^2 - 2q} - i \sin(2l\sqrt{\lambda^2 - 2q})(\lambda^2 - q)}$$

$$(2.4) \quad T(\lambda) = -\frac{e^{-2i\lambda} \lambda \sqrt{\lambda^2 - 2q}}{\cos(2l\sqrt{\lambda^2 - 2q})\lambda\sqrt{\lambda^2 - 2q} - i \sin(2l\sqrt{\lambda^2 - 2q})(\lambda^2 - q)}$$

We will choose the initial solitary wave with velocity v satisfying $\sin(2l\sqrt{v^2 - 2q}) = 0$, which corresponds to the resonant tunneling condition.

3. NUMERICAL METHOD

To integrate numerically equation (1.1), we implement the finite element method proposed in the paper of Akrivis et al [5], which was devoted to the study of the structural properties of blow-up solutions the NLS equation. (This method was also used in [12].) We consider an initial conditions in the form of solitary wave with phase $\phi_0 = 0$

$$(3.1) \quad u(x, 0) = Ae^{ivx} \operatorname{sech}(A(x - a_0))$$

approaching from the left ($a_0 \ll 0$) with velocity v . Without loss of generality, we set $A = 1$. The spatial domain of integration $[-L, L]$ (L is chosen large enough) is discretized with a uniform mesh $-L \leq x_0, x_1, \dots, x_N \leq L$. The basis for the Galerkin method are the ‘hat functions’ $\{\psi_1, \psi_2, \dots, \psi_N\}$ defined as

$$\psi_k(x) = \begin{cases} \frac{1}{h}(x - x_{k-1}), & x_{k-1} < x < x_k, \\ \frac{1}{h}(x_{k+1} - x), & x_k < x < x_{k+1} \\ 0 & \text{otherwise.} \end{cases}$$

and

$$\psi_N(x) = \begin{cases} \frac{1}{h}(x - x_{N-1}), & x_{N-1} < x < x_N, \\ 0 & \text{otherwise.} \end{cases}$$

where $h = 2L/N$, and $k = 1, 2, \dots, N - 1$. The projection of the equation on the elements of the basis gives

$$(3.2) \quad i\langle u_t, \psi_k \rangle - \frac{1}{2}\langle \partial_x u, \partial_x \psi_k \rangle - q\langle uV, \psi_k \rangle + \langle |u|^2 u, \psi_k \rangle = 0.$$

Denoting by u_n the approximation of the solution at time $t_n = ndt$, and using a Crank-Nicholson scheme for the time discretization, the system becomes

$$(3.3) \quad i\left\langle \frac{u_{n+1} - u_n}{dt}, \psi_k \right\rangle - \frac{1}{2}\left\langle \partial_x \left(\frac{u_{n+1} + u_n}{2} \right), \partial_x \psi_k \right\rangle - q\left\langle \left(\frac{u_{n+1} + u_n}{2} \right) V, \psi_k \right\rangle \\ + \left\langle \left| \frac{u_{n+1} + u_n}{2} \right|^2 \frac{u_{n+1} + u_n}{2}, \psi_k \right\rangle = 0.$$

or equivalently, denoting $y_n = (u_{n+1} + u_n)/2$:

$$(3.4) \quad \langle y_n, \psi_k \rangle + i \frac{dt}{4} \langle \partial_x y_n, \partial_x \psi_k \rangle + i \frac{dt}{2} q \langle y_n V, \psi_k \rangle - i \frac{dt}{2} \langle |y_n|^2 y_n, \psi_k \rangle - \langle u_n, \psi_k \rangle = 0.$$

The nonlinear equation (3.4) is solved by iteration. We choose $y_n^0 = u_n$, and y_n^{m+1} is calculated from

$$(3.5) \quad \langle y_n^{m+1}, \psi_k \rangle + i \frac{dt}{4} \langle \partial_x y_n^{m+1}, \partial_x \psi_k \rangle + i \frac{dt}{2} q \langle y_n^{m+1} V, \psi_k \rangle = i \frac{dt}{2} \langle |y_n^m|^2 y_n^m, \psi_k \rangle + \langle u_n, \psi_k \rangle.$$

In the implementation of the method, we find that y_n^m typically converges after a few iterations with a precision of 10^{-6} . Rewriting (3.5) in a matrix form, it becomes

$$(3.6) \quad (A + i \frac{dt}{4} K + i \frac{dt}{2} q B) Y = F,$$

where the $N \times N$ matrices A and K have entries

$$A_{jk} = \langle \psi_j, \psi_k \rangle = \begin{cases} \frac{h}{6}, & k=j-1; \\ \frac{2h}{3}, & k=j; \\ \frac{h}{6}, & k=j+1. \end{cases}$$

$$K_{jk} = \langle \partial_x \psi_j, \partial_x \psi_k \rangle = \begin{cases} -\frac{1}{h}, & k=j-1; \\ \frac{2}{h}, & k=j; \\ -\frac{1}{h}, & k=j+1. \end{cases}$$

Y is a the N -vector of components $Y_j = \langle y_n^{m+1}, \psi_j \rangle$, and the right hand side F is the N -vector of components

$$F_j = i \frac{dt}{2} \langle |y_n^m|^2 y_n^m, \psi_j \rangle + \langle u_n, \psi_j \rangle.$$

In the case of the $2\text{-}\delta$ potential (P1), the matrix B has the form:

$$B_{jk} = \psi_j(-l)\psi_k(-l) + \psi_j(l)\psi_k(l) = \begin{cases} 1, & \text{when } j = k = \frac{N}{2} + \frac{l}{h}; \\ 1, & \text{when } j = k = \frac{N}{2} - \frac{l}{h}; \\ 0, & \text{otherwise,} \end{cases}$$

where we choose the number of meshes, N , such that $\frac{l}{h}$ is an integer. while for the box potential (P2), $B = A\tilde{B}$, where matrix \tilde{B} has entries:

$$\tilde{B}_{jk} = \begin{cases} 1, & \text{when } \frac{N}{2} - \frac{l}{h} \leq j = k \leq \frac{N}{2} + \frac{l}{h}; \\ 0, & \text{otherwise.} \end{cases}$$

To check the precision of our calculations, we computed the invariants of the NLS equation, the mass, $M = \int_{\mathbb{R}} |u|^2 dx$ and the energy E that takes the form

$$E_{delta} = \int_{\mathbb{R}} \left(\frac{1}{2} |\nabla u|^2 - \frac{1}{2} |u|^4 \right) dx + q(|u(-l)|^2 + |u(l)|^2)$$

$$E_{box} = \int_{\mathbb{R}} \left(\frac{1}{2} |\nabla u|^2 - \frac{1}{2} |u|^4 \right) dx + \int_{-l}^l q |u(x)|^2 dx$$

	time	M	E_{δ}
Pre-Interaction	0	2.0000	554.8315
Interaction begins	0.3733	2.0000	554.9013
Interaction	0.4242	2.0000	555.1183
Interaction ends	0.4752	2.0000	554.9805
Post-Interaction	0.8486	2.0000	554.8316

TABLE 1. Conservation mass and energy (2- δ potential (P1))

	time	M	E_{box}
Pre-Interaction	0	2.0000	1.8459×10^3
Interaction begins	0.1860	2.0000	1.8476×10^3
Interaction	0.2325	2.0000	1.8695×10^3
Interaction ends	0.2791	2.0000	1.8478×10^3
Post-Interaction	0.4653	2.0000	1.8459×10^3

TABLE 2. Conservation of mass and energy (box potential (P2))

for the two examples of potentials we consider.

In our computations, we choose the size of the domain to be $[-L, L]$ with $L = 20$, and typically $N = 16000$ mesh points. The initial solution is centered at $a_0 = -10$. For the 2- δ potential (P1), the location of the barriers are at $\pm l$, $l = 0.05$, while the box potential (P2) is located at $[-l, l]$, with $l = 0.05$.

In Table 1 and 2, we show the value of the mass and energy of the solutions of the NLS equation with potentials (P1) and (P2) respectively. In the former case, the initial velocity is assumed to satisfy $\frac{v}{q} = -\tan(2lv)$ and we choose $v = q = \frac{15\pi}{2}$, and a time step $dt = 1.7 \times 10^{-4}$. In the latter case, v satisfies $2l\sqrt{v^2 - 2q} = n\pi$ and we choose $q = 10v$, $n = 1$, $v \approx 42.97$, and $dt \approx 10^{-4}$. Comparing the precision of the calculation with potential (P1) and (P2), we see that the singularities of the 2- δ potential lead to a stiffer problem, and thus less precision is expected.

We also validate our numerical code by reproducing the calculation presented in [12] for one delta potential. Figure 1 presents the convergence of the transmission rate $T_q^s(v) = \lim_{t \rightarrow \infty} \frac{\int_0^\infty |u(x,t)|^2 dx}{\int_{\mathbb{R}} |u(x,t)|^2 dx}$ to the expected asymptotic value $1/(1 + \alpha^2)$, where $\alpha = \frac{v}{q}$ for the values $\alpha = 0.6, 1, 1.4$. (Figure 2 of [12])

4. NUMERICAL RESULTS

4.1. Numerical Evidence of Resonant Tunneling. We now present the results of the numerical simulation of the NLS equation with potential (P1) and (P2), using the method presented in Section 3.

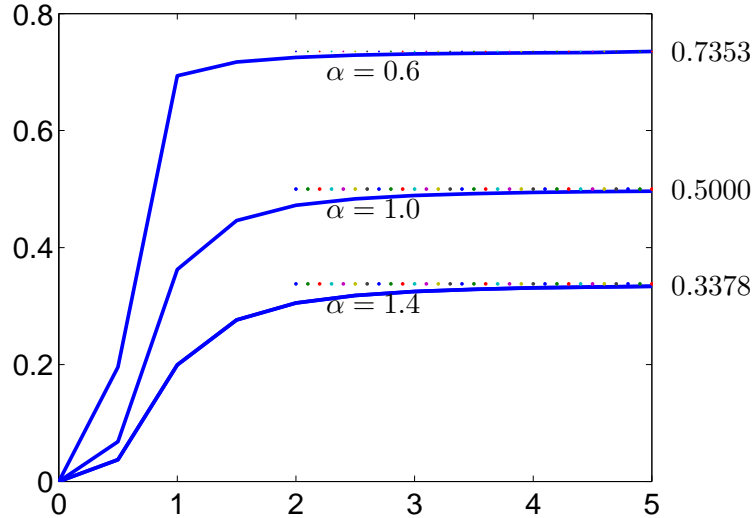


FIGURE 1. Convergence of $T_q^s(v)$ to the expected asymptotic value $1/(1 + \alpha^2)$ for $\alpha = \frac{v}{q} = 0.6, 1, 1.4$ as $v \rightarrow \infty$.

Figure 2 shows the evolution of the initial condition (3.1) in the case of the potential (P1). The velocity v is chosen to satisfy the equation $\frac{v}{q} = -\tan(2lv)$, and we choose $v = q = 12.5\pi$, $l = 0.03$ and $dt = 1.7 \times 10^{-4}$. The first panel (a) represents the initial solitary wave. The second and third (b, c) shows the interaction of the solitary wave with the barriers, at time $t = 0.19975, 0.29975$. Finally, the last panel (d) at time $t = 0.5$ is the transmitted wave in the post-collision phase. We see that for this choice of parameters, most of the wave is transmitted, and a small fraction of it is reflected. To describe this dynamics more precisely, define the transmission rate

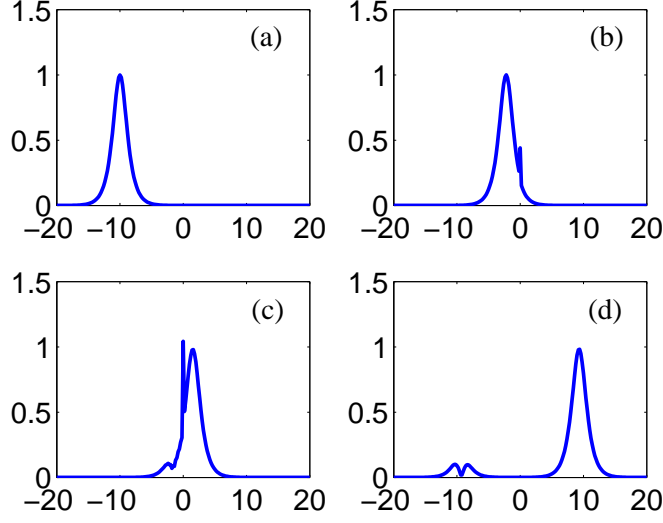
$$(4.1) \quad T_q^s(v) = \frac{\int_l^\infty |u(x, t)|^2 dx}{\int_{\mathbb{R}} |u(x, t)|^2 dx}$$

and the reflection rate,

$$(4.2) \quad R_q^s(v) = \frac{\int_{-\infty}^{-l} |u(x, t)|^2 dx}{\int_{\mathbb{R}} |u(x, t)|^2 dx}$$

where the total mass is $\int_{\mathbb{R}} |u(x, t)|^2 dx = 2$, we find that at time $t = 0.5$ (corresponding to the last panel of Figure 2), $T_q^s(v) = 0.9866$.

Table 3 shows that R_q^s and T_q^s for $l = 0.05, q = v$ and different values $v = \frac{(n-1/4)\pi}{2l}, n \in \mathbb{Z}$ for $n = 1, 2, 3, 4, 5$. As v increases, T_q^s tends to 1 and R_q^s tends to 0.

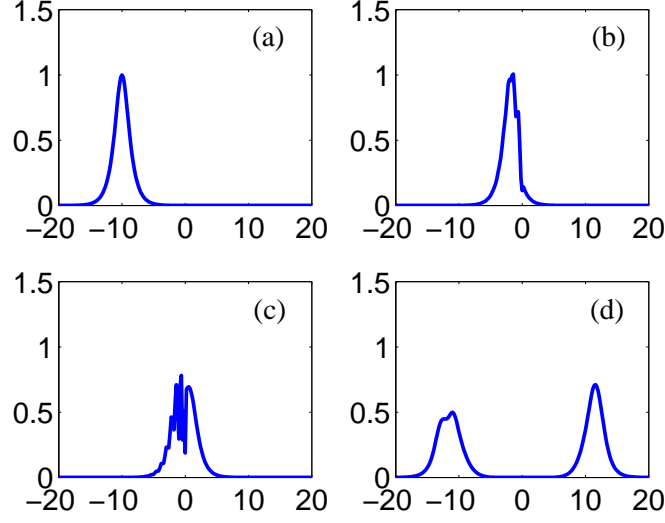
FIGURE 2. Resonant tunneling ($2 - \delta$ potential (P1))

n	v	T_q^s	R_q^s
1	23.5619	0.96557	0.03443
2	54.9778	0.97167	0.02833
3	86.3938	0.97322	0.02678
4	117.809	0.97393	0.02607
5	149.225	0.97435	0.02565

TABLE 3. Transmission and reflection rate, T_q^s and R_q^s , for potential (P1) with parameters $l = 0.05$ and $v = q$.

In contrast, when v, q do not satisfy the relation $\frac{v}{q} = -\tan(2lv)$, resonant tunneling does not occur. Figure 3 shows the time evolution of the solitary wave when $v = 8.75\pi$, $q = 40$, $l = 0.1$ and $dt \approx 2 \times 10^{-4}$. The wave clearly splits into 2 waves and the transmission rate is $T_p^s(v) = 0.5851$.

We repeat this numerical calculation with potential (P2). Choosing v, q such that $2l\sqrt{v^2 - 2q} = \pi$, namely, $q = 10v$, $v \approx 42.97$, $l = 0.05$ and $dt \approx 10^{-5}$, resonant tunneling occurs. Figure 4 represents the three regimes of the dynamics, at $t = 0$, $t = 0.1976$, $t = 0.26743$, and $t = 0.4655$. At the last time, the transmission rate is $T_q^s(v) = 0.9987417$. In contrast, Figure 5 shows the splitting of the wave when the resonant condition is not met: $v = \sqrt{(5\pi)^2 + 400}$, $q = 200$, $l = 0.05$ and $dt \approx 2 \times 10^{-4}$. The four panel of Figure 5 are the solitary wave at $t = 0, 0.319, 0.479, 0.8$, and the transmission rate is $T_p^s(v) = 0.75$ in the last panel.


 FIGURE 3. Splitting of the soliton ($2 - \delta$ potential (P1))

n	v	T_q^s	R_q^s
1	42.9691	0.99874	1.2583×10^{-3}
2	73.6227	0.99923	0.7687×10^{-3}
3	104.776	0.99929	0.7107×10^{-3}
4	136.061	0.99930	0.6950×10^{-3}
5	167.397	0.99931	0.6869×10^{-3}

 TABLE 4. Transmission and reflection rate, T_q^s and R_q^s , for potential (P2) with parameters $l = 0.05$ and $q = 10v$.

Table 4 shows the values of R_q^s and T_q^s for $l = 0.05$ and different values of v satisfying the resonant tunneling condition $l = \frac{n\pi}{2\sqrt{v^2-2q}}$, $n \in \mathbb{Z}$.

4.2. Resolution of Outgoing Waves. We identify the transmitted wave to a soliton corresponding to the initial condition (3.1) but with additional phase shift ϕ_1 , namely

$$(4.3) \quad u_{\phi_1}(x, t) = A \operatorname{sech}(A(x - a_0 - vt)) e^{i\phi_1 + ivx + i\frac{(A^2 - v^2)t}{2}}$$

To find the phase shift, we fix the initial speed v and the time t_1 so that t_1 is large enough for the wave to pass the barriers, and find ϕ_1 that minimizes

$$\|u(x, t_1) - u_{\phi_1}(x, t_1)\|_{L_x^\infty}$$

where $u(x, t_1)$ is the numerical solution.

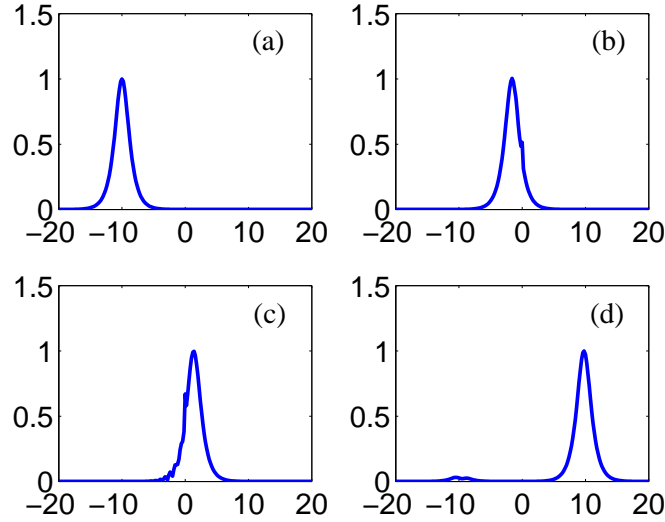


FIGURE 4. Resonant tunneling (box potential (P2))

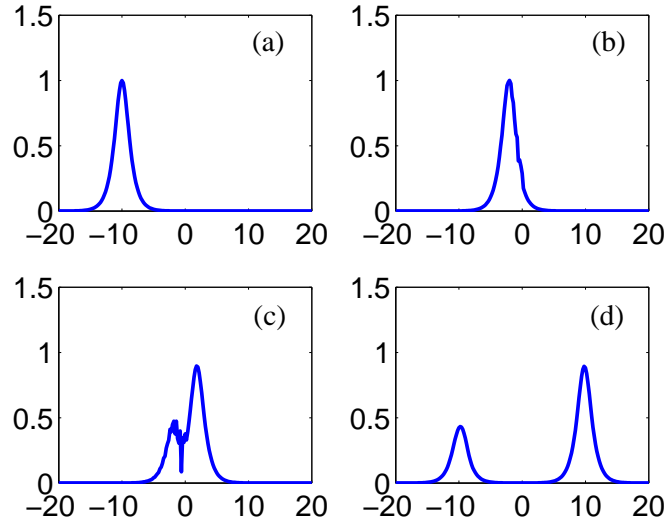


FIGURE 5. Splitting of the soliton (box potential (P2))

Denoting t_1 and t_2 the times where the center of the solitary wave is located at $x = 5$ and $x = 10$, respectively, we evaluate the difference

$$e = \max_{t \in [t_1, t_2]} \|u(x, t) - u_{\phi_1}(x, t)\|_{L_x^2}$$

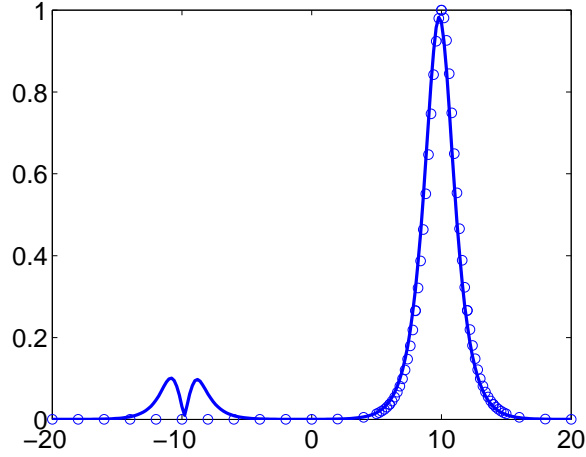


FIGURE 6. Superposition of the transmitted wave to the NLS soliton at time $t_2 = 0.5$; $|u(x, t)|$ is plotted with solid line and $|u_{\phi_1}(x, t)|$ is plotted with circles ($2\text{-}\delta$ potential (P1)).

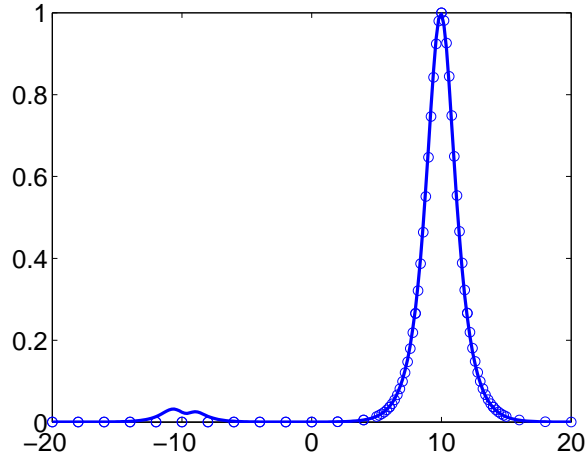


FIGURE 7. Superposition of the transmitted wave to the NLS soliton at time $t_2 = 0.4655$; $|u(x, t)|$ is plotted with solid line and $|u_{\phi_1}(x, t)|$ is plotted with circles (box potential (P2)).

to show how well the transmitted wave is approximated by the shifted soliton.

Figure 6 shows $|u(x, t)|$ (solid line) and $|u_{\phi_1}(x, t)|$ (circle) at $t = t_2$ for the $2\text{-}\delta$ potential, using the parameters as in Figure 2. We find $e \approx 0.1416$. Figure 7 shows the same result at $t = t_2$ for the box potential (P2) with parameters as in Figure 4 and we get $e \approx 0.0505$.

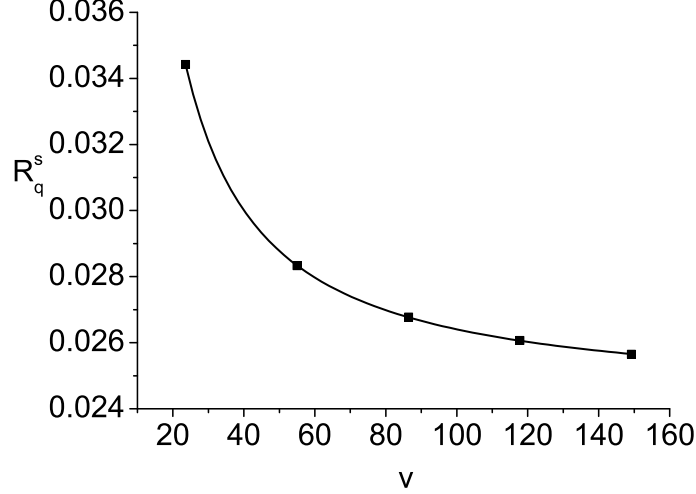


FIGURE 8. R_q^s is plotted with circles and the solid line is the graph of the asymptotic formula (4.4), with $\alpha = 1.08139$, $\beta = 0.30909$ and $\gamma = 0.02428$.

l	α	β	γ
0.06	1.076	0.33816	0.0336
0.05	1.081	0.30909	0.0242
0.04	1.084	0.27001	0.0160

TABLE 5. Values of α, β and γ as l varies when $\frac{v}{q} = 1$.

4.3. Asymptotic Behavior of Reflection Rates. Following the analysis of [4], we examine the dependence of the reflection rate $R_q^s(v)$ in terms of the velocity v , for various values of l and q and find

$$(4.4) \quad R_q^s(v) \approx \beta v^{-\alpha} + \gamma$$

Furthermore, the constant γ converges to 0, as l approaches to 0. We observe that the constant α in (4.4) is independent from l under 2- δ potential (P1) with a fixed ratio $\frac{v}{q}$.

For the potential (P1), we choose $l = 0.05$, $q = v$ and $v = \frac{(n-1/4)\pi}{2l}$, $n \in \mathbb{N}$, for $n = 1, 2, 3, 4, 5$. Fitting the data of Table 3 for $R_q^s(v)$ to a curve of the form $\beta v^{-\alpha} + \gamma$, we find $\alpha \approx 1.08139$, $\beta \approx 0.30909$ and $\gamma \approx 0.02428$ as indicated in Figure 8. Choosing different values of l , we show in Table 5 that γ decreases as l gets smaller, while α seems to keep the same value $\alpha \approx 1.08$.

l	α	β	γ
0.06	1.0624	0.07339	0.0082
0.05	1.0674	0.06451	0.0058
0.04	1.0699	0.05414	0.0037

TABLE 6. Values of α, β and γ as l varies when $\frac{v}{q} = \sqrt{3}$.

l	α	β	γ
0.06	1.196	1.54895	0.140
0.05	1.184	1.50725	0.108
0.04	1.176	1.42207	0.077

TABLE 7. Values of α, β and γ as l varies when $\frac{v}{q} = \frac{1}{\sqrt{3}}$.

Similar results are obtained for different values of the ratio $\frac{v}{q}$, namely $\frac{v}{q} = \sqrt{3}$ and $\frac{v}{q} = \frac{1}{\sqrt{3}}$, and shown in Table 6 and 7.

For the potential (P2), with $l = 0.05$ and the resonant tunneling condition $l = \frac{n\pi}{2\sqrt{v^2-2q}}, n \in \mathbb{Z}$, we obtain $\alpha \approx 3.54, \beta \approx 348$ and $\gamma \approx 0.00068$ by fitting the data in Table 4.

Acknowledgements CS acknowledges partial support from the Natural Sciences and Engineering Research Council of Canada grant 46179-05.

REFERENCES

- [1] W. K. Abou Salem. *Solitary wave dynamics in time-dependent potentials*, J. Math. Phys. **49**(2008), 032101.
- [2] W. K. Abou Salem. Effective dynamics of solitons in the presence of rough nonlinear perturbations. *Nonlinearity* 22: 747 - 763, 2009.
- [3] W. K. Abou Salem, J. Fröhlich and I. M. Sigal. *Collision of fast solitons for the nonlinear Schrödinger equation*, Commun. Math. Phys. **291**(2009), 151–176.
- [4] W.K. Abou Salem and C. Sulem, *Resonant tunneling of fast solitons through large potential barriers*, preprint.
- [5] G. D. Akrivis, V. A. Dougalis, O. A. Karakashian and W. R. McKinney, *Numerical approximation of blow-up of radially symmetric solutions of the nonlinear Schrödinger equation* SIAM J. Sci. Comput. **25** (2003), 186–212.
- [6] J. C. Bronski and R. L. Jerrard, *Soliton dynamics in a potential*, Math. Res. Lett., **7**(2000), 329–342.
- [7] J. Fröhlich, S. Gustafson, B. L. G. Jonsson, and I. M. Sigal, *Solitary wave dynamics in an external potential*, Commun. Math. Phys., **250**(2004), 613–642.
- [8] J. Fröhlich, T.-P. Tsai, and H.-T. Yau, *On the point-particle (Newtonian) limit of the non-linear Hartree equation*, Commun. Math. Phys., **225**(2002), 223–272.
- [9] J. Holmer and M. Zworski, *Slow soliton interaction with delta impurities*, J. Modern Dynamics**1**(2007), 689–718.
- [10] J. Holmer and M. Zworski, *Soliton interaction with slowly varying potentials*, IMRN ArtID 026, 36pp, 2008.
- [11] J. Holmer, J. Marzuola and M. Zworski, *Fast soliton scattering by delta impurities*, Commun. Math. Phys., **274**(2007), 187–216.

- [12] J. Holmer, J. Marzuola and M. Zworski, *Soliton splitting by external delta potentials*, Journal of Nonlinear Science, **17** (2007), 349–367.

DEPARTMENT OF MATHEMATICS, UNIVERSITY OF BRITISH COLUMBIA, VANCOUVER,
BC , CANADA

E-mail address: `walid@math.ubc.ca`

DEPARTMENT OF MATHEMATICS, UNIVERSITY OF TORONTO, TORONTO, ON, CANADA,
M5S 2E4

E-mail address: `xiaoliu@math.toronto.edu`

E-mail address: `sulem@math.toronto.edu`